Drifting dynamics of dense and sparse spiral waves in heterogeneous excitable media

Lida Xu,[1] Zhilin Qu,[2] and Zengru Di[1,*]
[1]*Department of Systems Science, Center for Complexity Research, Beijing Normal University, Beijing 100875, People's Republic of China*
[2]*Department of Medicine (Cardiology), University of California, Los Angeles, California 90095, USA*
(Received 3 November 2008; published 31 March 2009)

Spiral wave is shown to drift in heterogeneous excitable media, yet the dynamics remains incompletely understood. In this study, we investigated the effects of heterogeneities in excitable media on the drifting behaviors of dense and sparse spiral waves. Dense spiral waves occur in media of normal excitability and sparse spiral waves in media of low excitability. We numerically simulated the spiral wave drifting in a reaction-diffusion system with the Barkley kinetics and showed that dense and sparse spiral waves drifted differently under the same heterogeneous medium. To understand the drifting behaviors, we developed a kinematic model to describe the tip properties of the spiral waves under different conditions and showed that the kinematic model could well recapitulate the results observed in the reaction-diffusion system.

DOI: 10.1103/PhysRevE.79.036212 PACS number(s): 05.45.−a, 82.40.Ck, 47.32.C−

I. INTRODUCTION

Spiral waves are widely encountered patterns in excitable media, including heart muscle [1,2], aggregate of slime mold [3], and autocatalytic chemical reactions, such as the Belousov-Zhabotinsky (BZ) reaction [4,5]. Spiral wave drift induced by different external fields, such as illumination [6], electric field [7–13], and magnetic field [14], has been shown experimentally and theoretically. In the presence of a uniform electric field, spiral waves in the BZ reaction drift with a velocity whose perpendicular component to the electric field changes sign with chirality of the spiral wave [15,16]. An interesting phenomenon first shown by Krinsky *et al.* [17] is that dense and sparse spiral waves drift in opposite directions under the same electric field. In a previous study [18], we developed a kinematic model to investigate how this phenomenon occurs.

Spiral wave drift has also been shown in excitable media (or cardiac tissue) with either electrical or structural heterogeneities [19–21]. Several studies [13,16,19] have shown that a spiral wave in a heterogeneous medium always drifts toward the territory with longer refractory period (or equivalently longer cycle length of the spiral wave). However, how different heterogeneous structures affect spiral wave drift and what different drifting behaviors of dense and sparse spiral waves remain to be elucidated. In this study, we first use numerical simulation to investigate the drifting behaviors of dense and sparse spiral waves in different heterogeneous media. We then develop a kinematic model to investigate the mechanisms of the different drifting behaviors.

II. DRIFT OF DENSE AND SPARSE SPIRAL WAVES IN HETEROGENEOUS MEDIA

We use the following two-dimensional (2D) reaction-diffusion model of excitable medium to study the spiral wave behaviors:

$$\frac{\partial u}{\partial t} = f(u,v) + \nabla^2 u,$$

$$\frac{\partial v}{\partial t} = g(u,v), \tag{1}$$

where $f(u,v)$ and $g(u,v)$ are the local kinetics for which we use the Barkley model [22,23],

$$f(u,v) = \frac{1}{\varepsilon}u(1-u)\left(u - \frac{v+b}{a}\right), \quad \varepsilon \ll 1,$$

$$g(u,v) = u - v. \tag{2}$$

Equation (1) is integrated by an explicit Euler method with no-flux boundary conditions on a grid of 128×128 elements with $\Delta t = 0.002\,44$ and $L = 40$. The results maintain as the same if we increase the lattice to 256×256 elements [24].

By varying the parameters in Eq. (2), one can obtain different spiral wave behaviors in a homogeneous medium, including dense and sparse spiral waves [17]. Figure 1(A) shows a dense spiral wave for which the parameters are $a = 1.0$, $b = 0.03$, and $\varepsilon = 0.02$, while Fig. 1(B) shows a sparse spiral wave for which the parameters are $a = 0.55$, $b = 0.05$, and $\varepsilon = 0.02$. Unless otherwise noted, our simulations in this paper are under these parameter sets (except ε being a func-

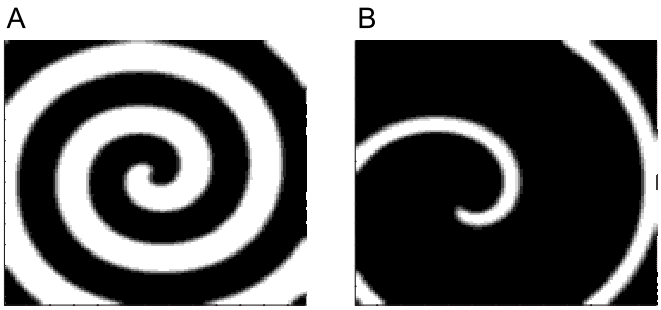

FIG. 1. (A) A dense and (B) a sparse spiral wave. The variable u is plotted in white when it is greater than 0.04.

*Author to whom correspondence should be addressed; zdi@bnu.edu.cn

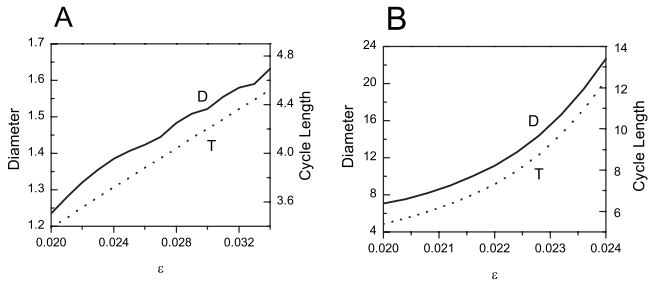

FIG. 2. Cycle length T (dashed lines) and core diameter D (solid lines, in unit of grid element) versus ε for (A) the dense and (B) the sparse spiral waves.

tion of space in heterogeneous media) and the spiral wave rotates in the clockwise direction, as shown in Fig. 1.

In Fig. 2, we show the core diameter (D) and the cycle length (T) of the spiral wave versus ε for the dense [Fig. 2(A)] and sparse [Fig. 2(B)] spiral waves in a homogeneous medium. The core is determined as described in a previous study [18]. For the dense spiral wave, both D and T increase almost linearly with ε for which we fit them by

$$D = (0.73 + 26.47\varepsilon) \times 40/128,$$

$$T = 1.78 + 80.84\varepsilon. \tag{3}$$

For the sparse spiral wave, both D and T increase with ε nonlinearly, and we fit them by

$$D = (-1.24e^3 + 1.8e^5\varepsilon - 9.2e^6\varepsilon^2 + 1.5e^8\varepsilon^3) \times 40/128,$$

$$T = -596.5 + 8.8e^4\varepsilon - 4.3e^6\varepsilon^2 + 7.2e^7\varepsilon^3. \tag{4}$$

Since the sparse spiral wave is due to low excitability of the medium, the diameter and cycle length of the sparse spiral wave are larger than those of the dense spiral wave.

To investigate the drifting behaviors of dense and sparse spiral waves in heterogeneous media, we first study the effects of moderate heterogeneities which are modeled by changing the parameter ε linearly in space along the x axis, i.e.,

$$\varepsilon = \varepsilon_0(1 + \delta x). \tag{5}$$

Since the cycle length T increases with ε, then in the heterogeneous tissue, T increases with x. In Fig. 3(A), we show two tip trajectories for a dense spiral wave with different ε_0 but the same δ. Under both conditions, the spiral wave drifts toward the longer cycle length territory but with opposite perpendicular components. In Fig. 3(B), we show two tip trajectories of a sparse spiral wave with different δ but the same ε_0. In this case, the spiral wave drifts toward the shorter cycle length territory if the gradient is small, but toward the longer cycle length territory if the gradient is large.

We also study spiral wave drift behaviors in medium in which ε is changed in space with a step function. Because of the diffusive coupling, the gradient of refractoriness changes continuously but steeply. Since the refractoriness in other area is almost uniform except in the border region, spiral wave drift occurs only when the spiral wave is near the border region. Figure 4(A) shows the tip trajectory for a dense spiral wave which drifts across the border from the region of short cycle length to the region of long cycle length and eventually stays in that region. However, a sparse spiral wave always migrates to the steep gradient region from either side and drifts along the border [as shown in Fig. 4(B)].

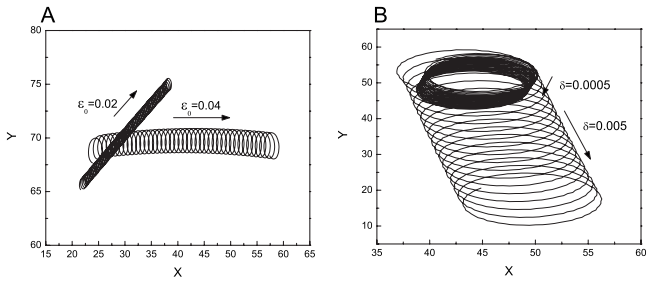

FIG. 3. Tip trajectories of (A) dense and (B) sparse spiral waves in heterogeneous media with ε increasing linearly along the x direction [Eq. (5)]. Panel (A) shows two different tip trajectories of a dense spiral wave with different ε_0 and the same δ=0.0125. Panel (B) displays two tip trajectories of a sparse spiral wave for different δ but the same ε_0=0.02. Arrows indicate the directions of drifting.

III. KINEMATIC MODEL FOR SPIRAL TIP DYNAMICS

In a previous study, we developed a kinematic model for spiral wave drift under an electric field [18], which can well capture the different drifting behaviors of dense and sparse spiral waves under the same electric field. In the present study, we extend our previous model to study spiral wave tip dynamics in heterogeneous medium. Figure 5 shows a schematic diagram of a stable spiral wave in a homogeneous medium. The spiral tip (point Q) traces a circle in the medium with a velocity c_n. The relation among c_n, the rotation period T, and the core radius R_c is $c_n = 2\pi R_c/T$. The radial velocity $c_g = 0$ for a stable spiral wave.

Based on the schematic plot in Fig. 5, one can describe the tip motion using the following differential equations:

$$\dot{x} = c_g \cos\theta - hc_n \sin\theta,$$

$$\dot{y} = c_g \sin\theta + hc_n \cos\theta,$$

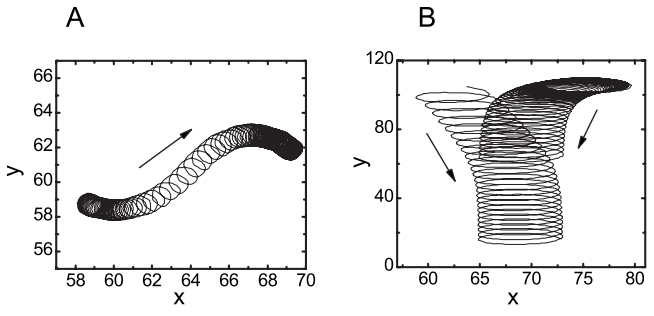

FIG. 4. Drifting behaviors of (A) a dense and (B) a sparse spiral wave when the parameter ε changes suddenly from ε=0.02 to ε=0.022 at grid x=64. Arrows indicate the directions of drift.

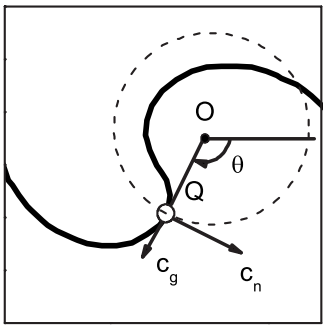

FIG. 5. A schematic diagram of a spiral wave in a homogeneous medium ($c_g=0$ for a stable spiral wave).

$$\dot{\theta} = h\omega, \tag{6}$$

where h is the chirality of the spiral wave ($h=+1$ for counterclockwise and $h=-1$ for clockwise).

In the homogeneous case, ε is uniform in space. As shown in Fig. 2, the core radius and rotation period are functions of ε, i.e., $R_c=R_c(\varepsilon)$ and $T_c=T_c(\varepsilon)$. The conduction velocity of point Q satisfies $c_n=V_c(\varepsilon)=2\pi R_c(\varepsilon)/T_c(\varepsilon)$. Therefore, as ε changes, all the quantities change accordingly.

When the medium is set to be heterogeneous by changing ε in space, i.e., $\varepsilon=\varepsilon(x,y)$, then the tip velocity, the instantaneous rotation period and radius change as the spiral wave rotates. If the velocity of the spiral tip is $\vec{V}$, then during a unit time interval, the displacement of the tip is $\Delta\vec{r}=\vec{V}$. Due to this displacement, the parameter ε at the tip also changes to $\varepsilon+\Delta\varepsilon$ with $\Delta\varepsilon=\vec{\nabla}\varepsilon\cdot\Delta\vec{r}=\vec{\nabla}\varepsilon\cdot\vec{V}$, and the instantaneous rotating period T and the normal velocity c_n of the tip will be changed accordingly based on the above relationships. For example, the change in the instantaneous rotation period is $\Delta T_c=T_c'(\varepsilon)\Delta\varepsilon=T_c'(\varepsilon)\vec{\nabla}\varepsilon\cdot\vec{V}$. Based on the drift of the spiral wave and continuous changes in parameters, we assume that the normal velocity of the spiral tip c_n and the instantaneous rotation period T in the heterogeneous medium are

$$c_n(\varepsilon+\Delta\varepsilon) = V_c(\varepsilon) + \lambda\Delta V_c = V_c(\varepsilon) + \lambda V_c'\vec{\nabla}\varepsilon\cdot\vec{V}, \tag{7}$$

$$T(\varepsilon+\Delta\varepsilon) = T_c(\varepsilon) + \gamma\Delta T_c = T_c(\varepsilon) + \gamma T_c'\vec{\nabla}\varepsilon\cdot\vec{V}, \tag{8}$$

where λ and γ are two parameters. For a stable spiral wave in a homogeneous medium, the curvature of the spiral wave is time independent. However, in a heterogeneous medium, the spiral wave deforms as the spiral wave drifts, which changes the curvature of the wave front, causing a radial velocity c_g, as illustrated in Fig. 6.

According to the above discussion, due to the changes in the instantaneous rotation radius R_c and the conduction velocity V_c, a nonzero radial velocity c_g exists in the spiral tip. As shown in Fig. 6, the increase in rotation radius $\Delta R_c=R_{c2}-R_{c1}$ would have a positive effect on radial speed. In contrast, due to the limit propagation rate, the radial speed decreases when the corresponding velocity V_c increases. So we assume that the radial velocity is linearly proportional to those changes,

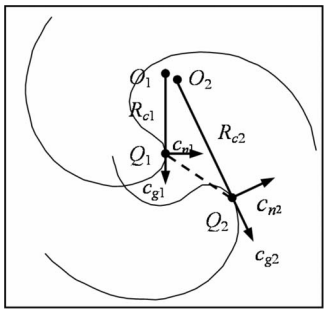

FIG. 6. A schematic diagram of a drifting spiral wave.

$$c_g = \rho\Delta R_c - \alpha\Delta V_c = (\rho R_c' - \alpha V_c')\vec{\nabla}\varepsilon\cdot\vec{V}, \tag{9}$$

where and in the following formulas, the prime appended to R_c, V_c, and T_c means their derivatives with respect to parameter ε. In addition to the change in c_g, the instantaneous angular velocity will also change. We assume it changes as follows:

$$\omega = \frac{2\pi}{T} - \beta\frac{c_g}{c_n}. \tag{10}$$

In Eqs. (7)–(10), λ, γ, ρ, α, and β are adjustable parameters.

With the presence of both normal velocity c_n and radial velocity c_g, the velocity of the spiral tip is

$$\vec{V} = c_n\hat{n} + c_g\hat{r}. \tag{11}$$

From Eqs. (7), (8), and (11), we have

$$\vec{\nabla}\varepsilon\cdot\vec{V} = \frac{V_c\vec{\nabla}\varepsilon\cdot\hat{n}}{1-\lambda V_c'\vec{\nabla}\varepsilon\cdot\hat{n}-(\rho R_c'-\alpha V_c')\vec{\nabla}\varepsilon\cdot\hat{r}}. \tag{12}$$

In the numerical simulations, we assumed that the parameter gradient was in the x direction, i.e., $\vec{\nabla}\varepsilon=\varepsilon'\hat{i}$, where ε' means its derivative with respect to the space variable x, and the spiral wave is rotating clockwise. So we have

$$\vec{\nabla}\varepsilon\cdot\vec{V} = \frac{V_c\varepsilon'\sin\theta}{1-\lambda V_c'\varepsilon'\sin\theta-(\rho R_c'-\alpha V_c')\varepsilon'\cos\theta}, \tag{13}$$

and

$$c_n = \frac{V_c[1-(\rho R_c'-\alpha V_c')\varepsilon'\cos\theta]}{1-\lambda V_c'\varepsilon'\sin\theta-(\rho R_c'-\alpha V_c')\varepsilon'\cos\theta}, \tag{14}$$

$$c_g = \frac{V_c(\rho R_c'-\alpha V_c')\varepsilon'\sin\theta}{1-\lambda V_c'\varepsilon'\sin\theta-(\rho R_c'-\alpha V_c')\varepsilon'\cos\theta}, \tag{15}$$

$$\frac{c_g}{c_n} = \frac{(\rho R_c'-\alpha V_c')\varepsilon'\sin\theta}{1-(\rho R_c'-\alpha V_c')\varepsilon'\cos\theta}. \tag{16}$$

Combining Eqs. (8), (10), and (6), one can obtain the spiral wave drift behaviors under different conditions.

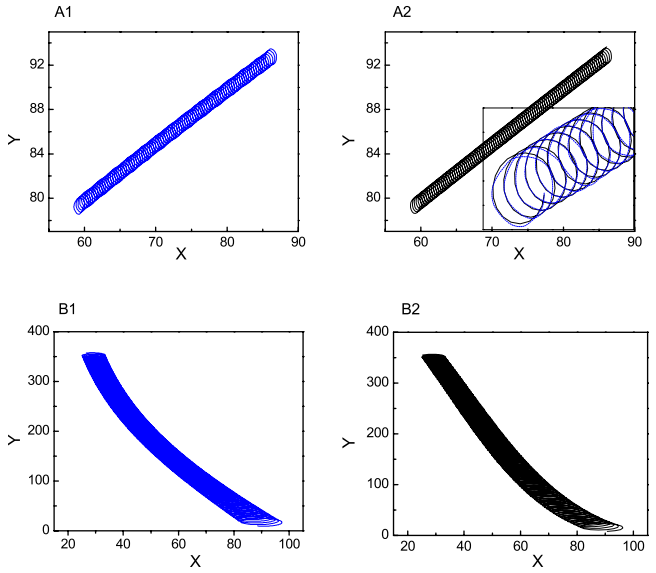

FIG. 7. (Color online) Tip trajectories of a dense (A1) and a sparse (B1) spiral wave from simulations and from the kinematic models (A2) and (B2). The gradients are $\varepsilon=0.02(1+0.0125x)$ [for (A)] and $\varepsilon=0.02(1+0.005x)$ [for (B)]. The parameter sets for the kinematic model are: dense (A2): $\alpha=52.5$, $\beta=2.63$, $\gamma=10$, $\lambda=10$, and $\rho=52.5$; sparse (B2): $\alpha=18$, $\beta=0.3$, $\gamma=1.56$, $\lambda=1.56$, and $\rho=3$. The inset of A2 shows a good agreement between the theoretical (dashed line) and simulation (solid line) results.

IV. COMPARISON OF NUMERICAL SIMULATION AND KINEMATIC MODEL

Figure 7 shows the tip trajectories of a dense (A1) and a sparse (B1) spiral wave in a medium with a linear gradient in ε and the corresponding results (A2 and B2) from the kinematic equations, showing a very good agreement. The trajectories from the kinematic equations are obtained by using the fitted radius $R[\varepsilon(x)]=D[\varepsilon(x)]/2$ and $T[\varepsilon(x)]$ from Eqs. (3) and (4) for the dense and sparse spiral waves, respectively. With the same set of parameters, we can predict the drifting velocities for different gradients (as shown in Fig. 8), and the results fit very well with the numerical simulations.

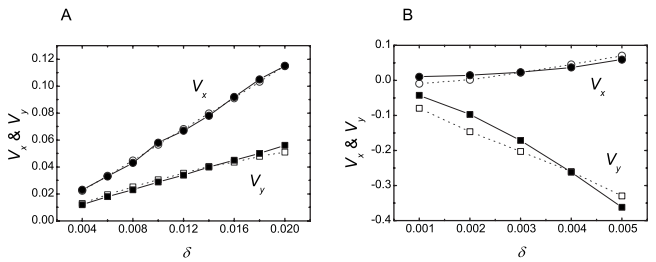

FIG. 8. x and y components of the drifting velocity versus linear gradient δ for (A) a dense and (B) a sparse spiral wave. Open symbols are from 2D spiral wave simulation and solid symbols are from kinematic model. We use the same sets of parameters as in Fig. 7. The initial conditions are: (A) $x=59.8$, $y=79.24$, and $\theta=0.0$; (B) $x=57.8$, $y=63$, and $\theta=\pi/3$.

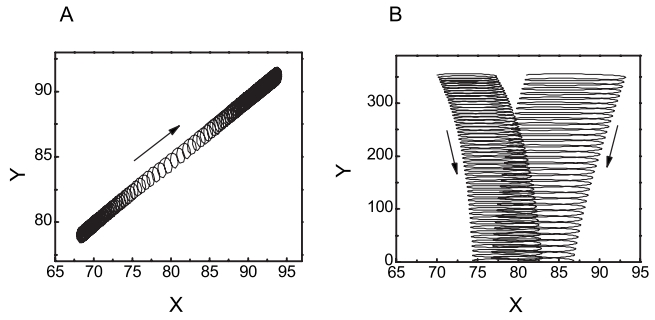

FIG. 9. Drifting behaviors of (A) a dense and (B) a sparse spiral wave from the kinematic model with parameter ε being a sigmoid function of x as follows (corresponding to simulation results in Fig. 4): (A) $\varepsilon=(0.02-0.024)/[1.0+\exp(\frac{x-80.0}{4.0})]+0.024$; (B) $\varepsilon=(0.02-0.022)/[1.0+\exp(\frac{x-80.0}{4.0})]+0.022$.

The model can also reproduce the drifting behaviors in the medium with step changes in parameters. Due to the diffusive coupling, the gradient of refractoriness, and thus the physical quantities such as the cycle length T changes continuously but steeply. So in our kinematic model, we set ε to be a sigmoidal function of x instead of a step function. Using the sigmoidal function, the kinematic model can reproduce the tip trajectories from the numerical simulations reasonably well (comparing Fig. 9 with Fig. 4).

We have also simulated a heterogeneous medium in which $\varepsilon=0.02$ in a circular region in the center of the medium and $\varepsilon=0.022$ for the rest of the medium. The parameters are set to sparse spiral wave regime as in Fig. 1(B). The spiral wave drifts along the border of circular regime [Fig. 10(A)]. Using the kinematical model, we obtain the same tip trajectory [Fig. 10(B)].

V. CONCLUSIONS

In this study we show that the drifting behaviors of dense and sparse spiral waves in heterogeneous medium are different. Based on the spiral tip properties of the spiral wave, we

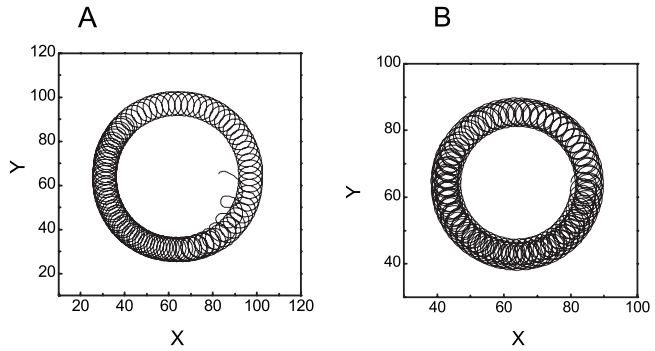

FIG. 10. Tip trajectories from (A) the numerical simulation and (B) the kinematic model for a sparse spiral wave in a medium with a circular heterogeneity. The border is given by a step change in parameter ε in (A) (as stated in the text) and by a sigmoid function in (B) as follows: $\varepsilon=(0.02-0.022)/[1.0+\exp(\frac{x-25.0}{5.0})]+0.022$ and $R=\mathrm{sqrt}[(x-64)^2+(y-64)^2]$.

develop a kinematic model to describe the dynamics of the tip trajectory, which can well capture the drifting dynamics observed in the reaction-diffusion equations. Since dense spiral waves occur in normal excitable medium and sparse spiral waves occur in low excitable medium, our study provides important information for spiral wave drifting dynamics in excitable medium and can provide insights into arrhythmias termination and maintenance in cardiac tissue.

[1] A. T. Winfree, Chaos **8**, 1 (1998).
[2] A. Garfinkel, Y.-H. Kim, O. Voroshilovsky, Z. Qu, J. R. Kil, M.-H. Lee, H. S. Karagueuzian, J. N. Weiss, and P.-S. Chen, Proc. Natl. Acad. Sci. U.S.A. **97**, 6061 (2000).
[3] F. Siegert and C. J. Weijer, Physica D **49**, 224 (1991).
[4] A. M. Zhabotinsky and A. N. Zaikin, *Oscillatory Processes in Biological and Chemical Systems* (Nauka, Pushchino, Russia, 1971), Vol. 2.
[5] A. T. Winfree, Science **175**, 634 (1972).
[6] H. Zhang, Z. Cao, N.-J. Wu, H.-P. Ying, and G. Hu, Phys. Rev. Lett. **94**, 188301 (2005).
[7] G. Hu, J. Xiao, L. O. Chua, and L. Pivka, Phys. Rev. Lett. **80**, 1884 (1998).
[8] W. Liu, J. Xiao, and J. Yang, Phys. Rev. E **72**, 057201 (2005).
[9] Q. Ouyang and H. L. Swinney, Nature (London) **352**, 610 (1991).
[10] A. T. Winfree, Phys. Lett. A **149**, 203 (1990).
[11] A. T. Winfree, Physica D **49**, 125 (1991).
[12] X. Zhang, M. Fu, J. Xiao, and G. Hu, Phys. Rev. E **74**, 015202 (2006).
[13] J.-X. Chen, H. Zhang, and Y.-Q. Li, J. Chem. Phys. **124**, 014505 (2006).
[14] J. Lee, J. Kim, G.-H. Yi, and K. J. Lee, Phys. Rev. E **65**, 046207 (2002).
[15] A. Belmonte and J. M. Flesselles, Europhys. Lett. **32**, 267 (1995).
[16] O. Steinbock, J. Schutze, and S. C. Muller, Phys. Rev. Lett. **68**, 248 (1992).
[17] V. Krinsky, E. Hamm, and V. Voignier, Phys. Rev. Lett. **76**, 3854 (1996).
[18] Z. Di, Z. Qu, J. N. Weiss, and A. Garfinkel, Phys. Lett. A **308**, 179 (2003).
[19] K. H. W. J. ten Tusscher and A. V. Panfilov, Am. J. Physiol. Heart Circ. Physiol. **284**, H542 (2003).
[20] Z. Qu and J. N. Weiss, Am. J. Physiol. Heart Circ. Physiol. **289**, H1692 (2005).
[21] Z. Di, D. Wang, Z. Cao, and Z. Qu, in Proceedings of International Conference on Neural Networks and Brain (ICNN&B '05), edited by M. S. Zhao and Z. Z. Shi, (IEEE Press, Beijing, China, 2005) Vol. 3, p. 1900.
[22] D. Barkley, Physica D **49**, 61 (1991).
[23] D. Barkley, Phys. Rev. Lett. **68**, 2090 (1992).
[24] A. V. Panfilov, R. H. Keldermann, and M. P. Nash, Proc. Natl. Acad. Sci. U.S.A. **104**, 7922 (2007).